remote sensing

MDPI

Article

A Case Study on Ground Subsidence and Backfill Deformation Induced by Multi-Stage Filling Mining in a Steeply Inclined Ore Body

Guang Li [1,2], Yang Wan [1,2,3], Jie Guo [1,2], Fengshan Ma [1,2,*], Haijun Zhao [1,2] and Zhiqing Li [1,2]

[1] Key Laboratory of Shale Gas and Geoengineering, Institute of Geology and Geophysics, Chinese Academy of Sciences, Beijing 100029, China
[2] Innovation Academy for Earth Science, Chinese Academy of Sciences, Beijing 100029, China
[3] College of Engineering and Technology, University of Chinese Academy of Sciences, Beijing 100049, China
* Correspondence: fsma@mail.iggcas.ac.cn

Abstract: The backfill mining method transports treated tailings to the mined-out area, which not only improves the surrounding environment of the mine but also enables the mined-out area to continue mining and production under the support of the filling body. However, with the growth in the depth and scale of mining, ground subsidence, and backfill deformation are becoming increasingly serious problems. As an example, in the Jinchuan mine, a typical multi-stage filling mining mine in China, the deformation law of surface rock mass and backfill are studied through a method combining field monitoring and numerical simulation. The major findings are as follows: (a) A settlement funnel is formed on the ground, and its radius gradually expands with continuous mining and filling. The location of the settlement center moves toward the surface above the footwall of the ore body, and the maximum subsidence reaches 739 mm in 14.5 years. (b) Three-section mining significantly affects the surface deformation, and the single subsidence center on the upper wall develops into the double subsidence center with the mining and filling. When the three-section mining is finished, the maximum value of the surface subsidence reaches about 1.35 m and the mining area is still in a relatively stable state. (c) The whole filling body presents obvious subsidence, with the development of the multi-stage mining and filling. Bed separation phenomena are found between the filling layers, and the closer to the interior, the more obvious it becomes. The backfill's subsidence characteristics are similar to the surface's; that is, both the subsidence amount and speed are higher on the hanging wall than on the footwall. (d) The backfill mainly shrinks inward in the horizontal direction, and the deformation is mainly manifested as an internal uplift and an external subsidence in the vertical direction. The mass instability of the backfill is difficult because of the insufficient deformation space, and the influence of large-scale deformation on the mining and overlying strata needs to be considered, as well as the local deformation near the rock contact zone surrounding the backfill. The results provide technical support for filling mining in the Jinchuan mine and provide a reference for other projects with similar engineering conditions.

Keywords: backfill mining method; multi-stage mining; Jinchuan mine; surface movement; filling body stability

Citation: Li, G.; Wan, Y.; Guo, J.; Ma, F.; Zhao, H.; Li, Z. A Case Study on Ground Subsidence and Backfill Deformation Induced by Multi-Stage Filling Mining in a Steeply Inclined Ore Body. *Remote Sens.* **2022**, *14*, 4555. https://doi.org/10.3390/rs14184555

Academic Editors: Alex Hay-Man Ng and Francesca Cigna

Received: 8 July 2022
Accepted: 9 September 2022
Published: 12 September 2022

1. Introduction

With the continuous development of the economy, the demand for resources is gradually increasing. As shallow resources are exhausted around the world, mining must advance deeper into the earth [1,2]. As a green mining method, the backfill method has been increasingly used [3,4]. The filling body supports the goaf together with the surrounding rock and controls the surface subsidence as a substitute for the ore body after cementing with the surrounding rock [5]. However, due to the continuous deterioration of the mining environment and the influence of multi-stage mining disturbances, serious

surface subsidence and collapse accidents still occur in mines using the backfill method [6]. Therefore, it is very important for mine safety to master the law of surface subsidence and backfill deformation in multi-stage mining.

The ground subsidence caused by underground mineral resources mining is not only a regional engineering geological disaster but also a complex rock-mechanics problem [7,8]. In terms of the risk assessment of mine-surface subsidence, some researchers analyze the risks according to historical deformation data, ground cracks, surface morphology, or surface building deformation [9,10]. Some researchers have adopted the statistical method, the grey correlation analysis method, the probability integration method, the fuzzy comprehensive evaluation method, the Geographic Information System (GIS), and other methods [11,12]. As for the mechanism of surface subsidence in metal mines, previous research results have shown that the extraction of underground minerals makes room for surrounding rock deformation, and the deformations are continuously transferred to the surface, which causes ground subsidence [13–17]. In terms of backfill stability, scholars have carried out a large number of studies on the material ratio, deformation characteristics, the failure law of the backfill through on-site monitoring, and laboratory tests [18–20]. It was found that the filling body absorbs and transfers the ground pressure and creates a supporting force at the same time after it is filled into the goaf, which is very helpful for stope stability [21–27]. Moreover, increasing mining times can greatly promote the balance of the backfill and surrounding rock, which can improve mine safety [28–30].

In sum, researchers have recognized that surface subsidence and backfill deformation are crucial to the overall stability of the mine and have carried out many studies on these issues, but there are still few studies performed in the multi-stage mining environment. Therefore, taking Jinchuan mine, a typical multi-stage filling mining mine, as an example, based on detailed field investigation, the deformation law of the surface rock mass and backfill are studied using a method combining field monitoring and numerical simulation. The results provide technical support for filling mining in the Jinchuan mine and provide a reference for other projects with similar engineering conditions.

2. The Study Area

Jinchuan mine, located in Gansu Province, China, is the third-largest copper–nickel deposit in the world and has high economic benefits and strategic significance [31]. Because it is located at the junction of tectonic units, this area has special engineering geological conditions such as intense tectonic movement, high in situ stress, developed rock fissures, and poor overall stability. The terrain is generally high in elevation in the north and low in the east, with a slope of 8–12°, and the average elevation is 1750 m [32].

As shown in Figure 1, the Jinchuan mine can be divided into four mining areas from west to east. As the object of this study, the orebody in mining area No. 3 is inclined to the southwest, with a dip angle of 25–65° and a total length of 1300 m. The maximum thickness of the orebody is about 120 m, and the top pinch-out end of the orebody is about 200 m from the surface [33].

Downward filling mining has been adopted in mining area No. 3 for several decades, resulting in the formation of a filling body with a huge volume in the goaf. In order to further improve the mining efficiency, several working faces have been set up, and the typical cutaway schematic drawing and mining sequence are shown in Figure 2. The height of a single section is 20 m, and each section is divided into five sublevels with heights of 4 m [34]. Single sub-level mining was used in stages 1, 2, and 4, while double sub-level mining was used in stage 2 and triple sub-level mining was used in stage 5. Under the influence of multi-stage mining disturbance, surface deformation and filling body destruction have been found in the study area. As a complex regional system, the stability of the ground rock mass and backfill under multi-stage mining is an important problem that the mine confronts.

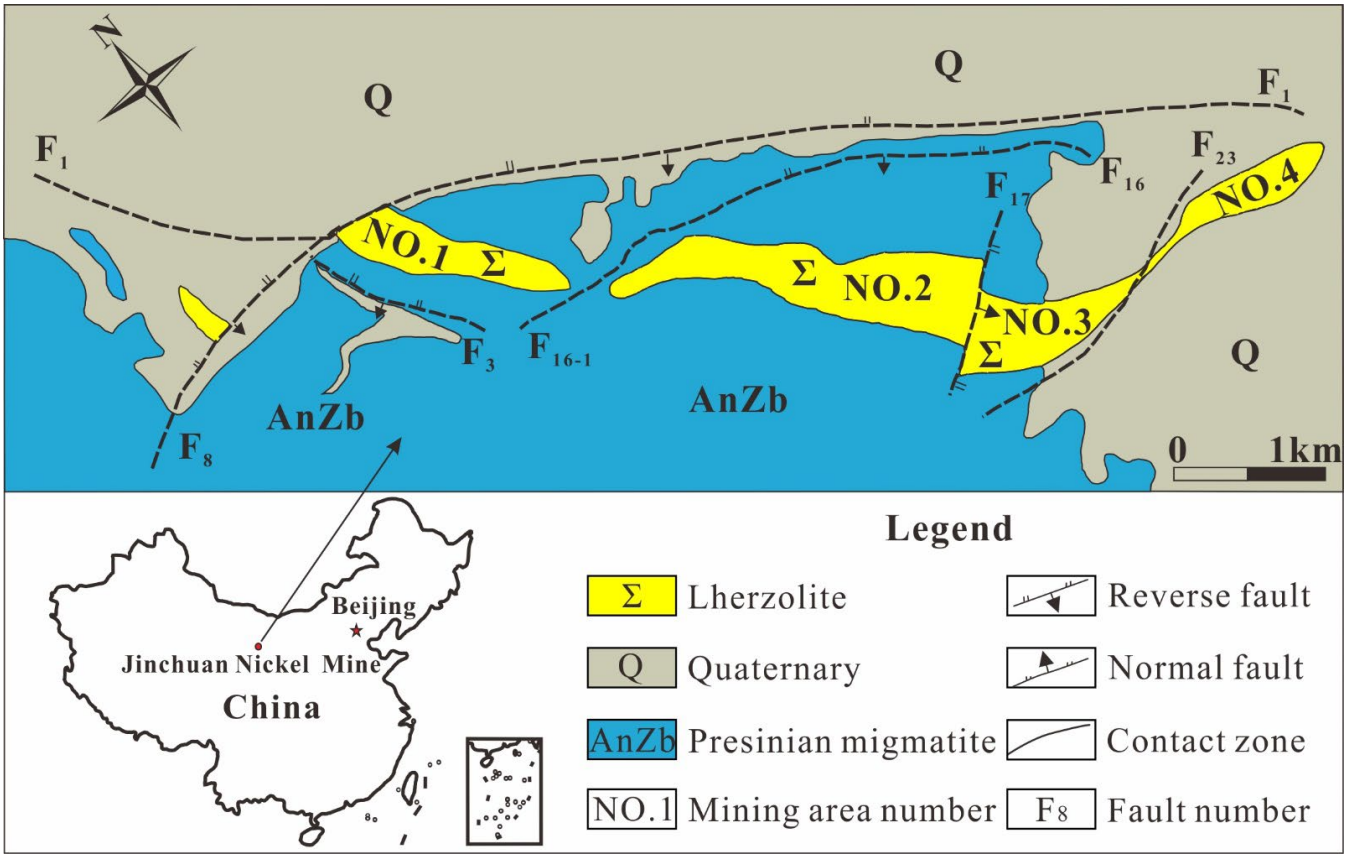

Figure 1. Engineering geologic map of Jinchuan Mine.

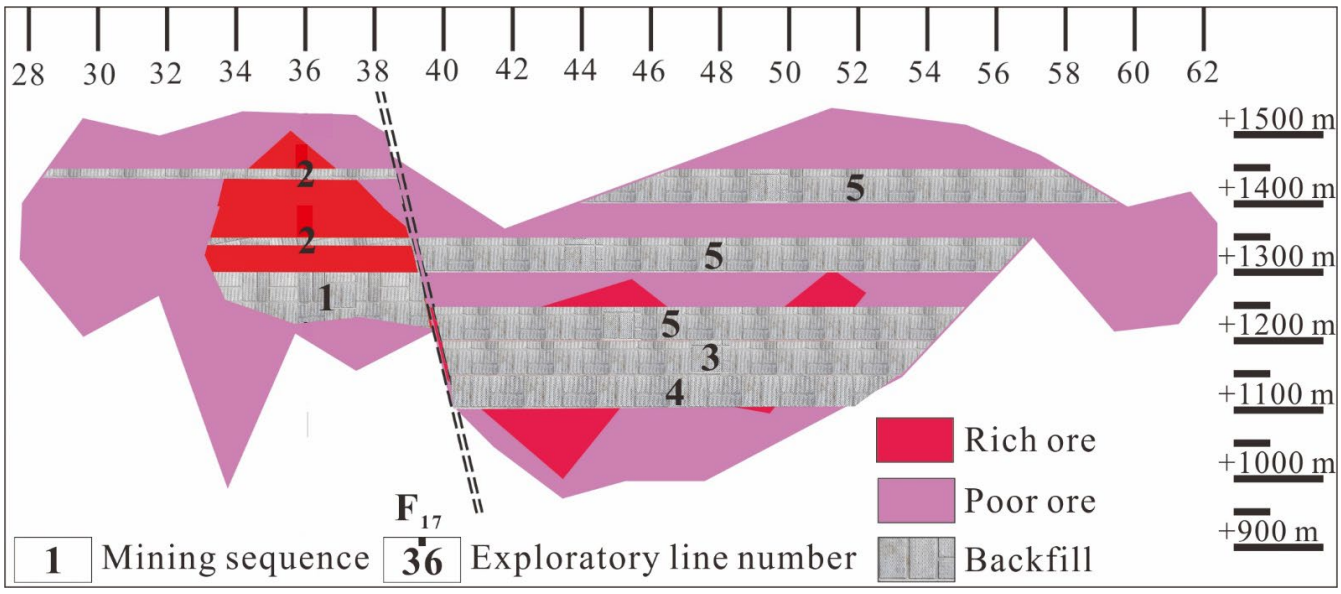

Figure 2. Cutaway schematic drawing and mining sequence.

3. Field Monitoring

3.1. Monitoring Method

Surface deformation data can objectively reflect the overall deformation characteristics of the mine. Historical subsidence records provide essential data to study subsidence evolution. A Global Navigation Satellite System (GNSS) monitoring technique has both high

precision and efficiency, making it suitable for the large-scale and real-time synchronous measurement of vertical and horizontal displacements in mining areas.

A GNSS monitoring system was set up in the study area in 2005, and the monitoring frequency was 6 months. Both a reference net and a deformation net are defined on the ground surface at the mine, and 229 monitoring points were set up along the dipping direction of the ore body. The reference net comprises seven benchmarks, which are all located on the firm bedrock, far away from the mining area.

Z-12-type receivers and antennas (Ashtech Inc., Sunnyvale, CA, USA) were used for subsidence monitoring. The nominal accuracy of the measurements of horizontal and vertical displacement was 3 mm ± 0.5 ppm and 5 mm ± 1 ppm, respectively. For each segment, the survey time lasted 1–2 h, while the data collection interval was 10 s. Horizontal and vertical displacements of each monitoring point were calculated for each measuring cycle using baseline processing, constraint network adjustments, and coordinate conversion.

3.2. Analysis of Surface Subsidence

Taking the monitoring results of the first phase as the base data, surface subsidence contour maps from 2005 to 2010 and 2005 to 2019 were drawn, as shown in Figure 3.

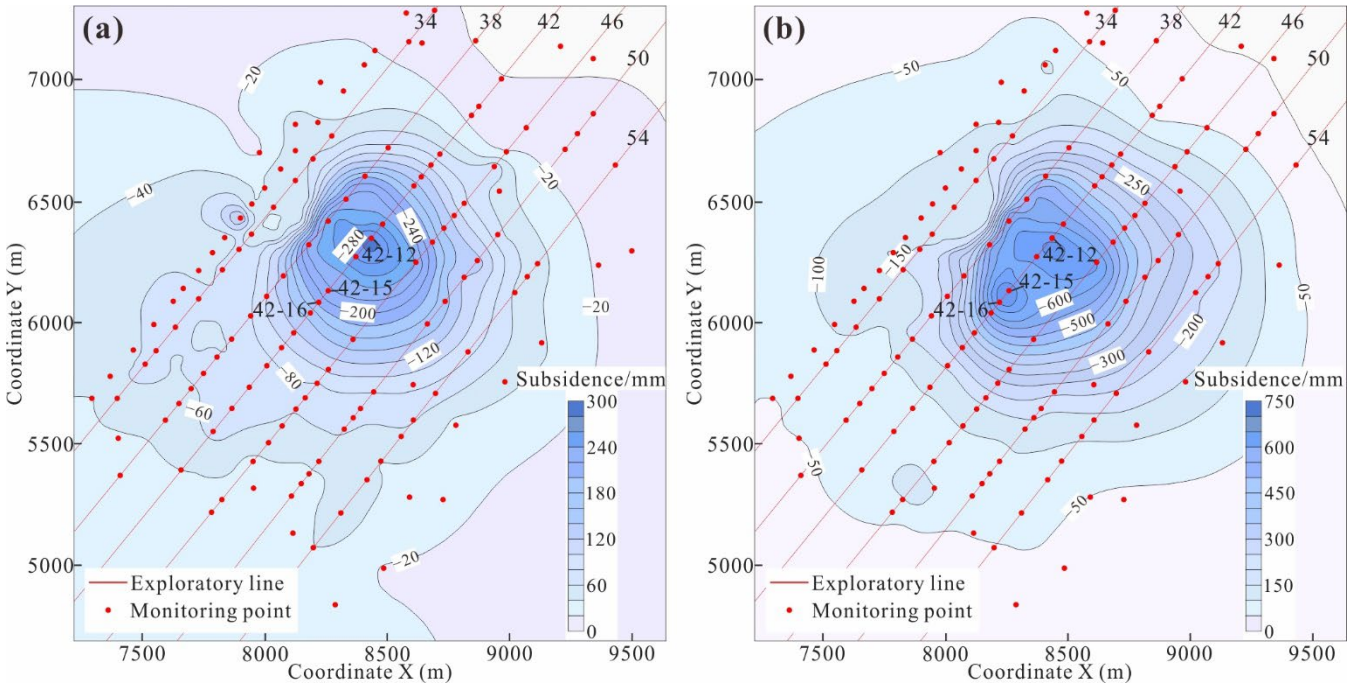

Figure 3. Contour map of surface subsidence (unit: mm). (**a**) Surface subsidence contour map from May 2005 to November 2010; (**b**) Surface subsidence contour map from May 2005 to November 2019.

It can be seen from the figure that most monitoring points gradually sink during the monitoring period, and a few points show an upward trend. With the mining advance, the accumulated settlement increases continuously, and the subsidence range of the mining area expands outward. The whole surface appears as a settlement funnel shape centered on the measuring point 42–12. The settlement of the measuring points near the orebody is obviously larger than that far away from the orebody, and the maximum subsidence reaches 739 mm in 14.5 years.

Comparing Figure 3a,b shows that the location of the settlement center had an apparent movement toward the surface above the footwall of the ore body. Meanwhile, a second settlement center was formed between monitoring points 42–15 and 42–16. With continuous excavation, the two settlement centers may melt into a large settlement center in the future. This may be related to the steeply dipping ore body: the settlement is first developed on the surface above the mining site.

3.3. Analysis of Backfill Deformation

In order to master the deformation of the large filling body, three groups of displacement gauges were installed on the +1200 m working plane, corresponding to lines 42, 44, and 46, which have serious surface subsidence. Considering that the backfill is cemented with a thickness of 5 m, there will also be differences in deformation between layers. Thus, three measuring points were designed in each group, with burial depths of 6 m, 10 m, and 14 m, as shown in Figure 4a. The equipment installed in each borehole is a JMDL3205 single-point displacement meter with an aperture of 30 mm. Through on-site data collection and indoor data processing, the deformation curves are shown in Figure 4b–d.

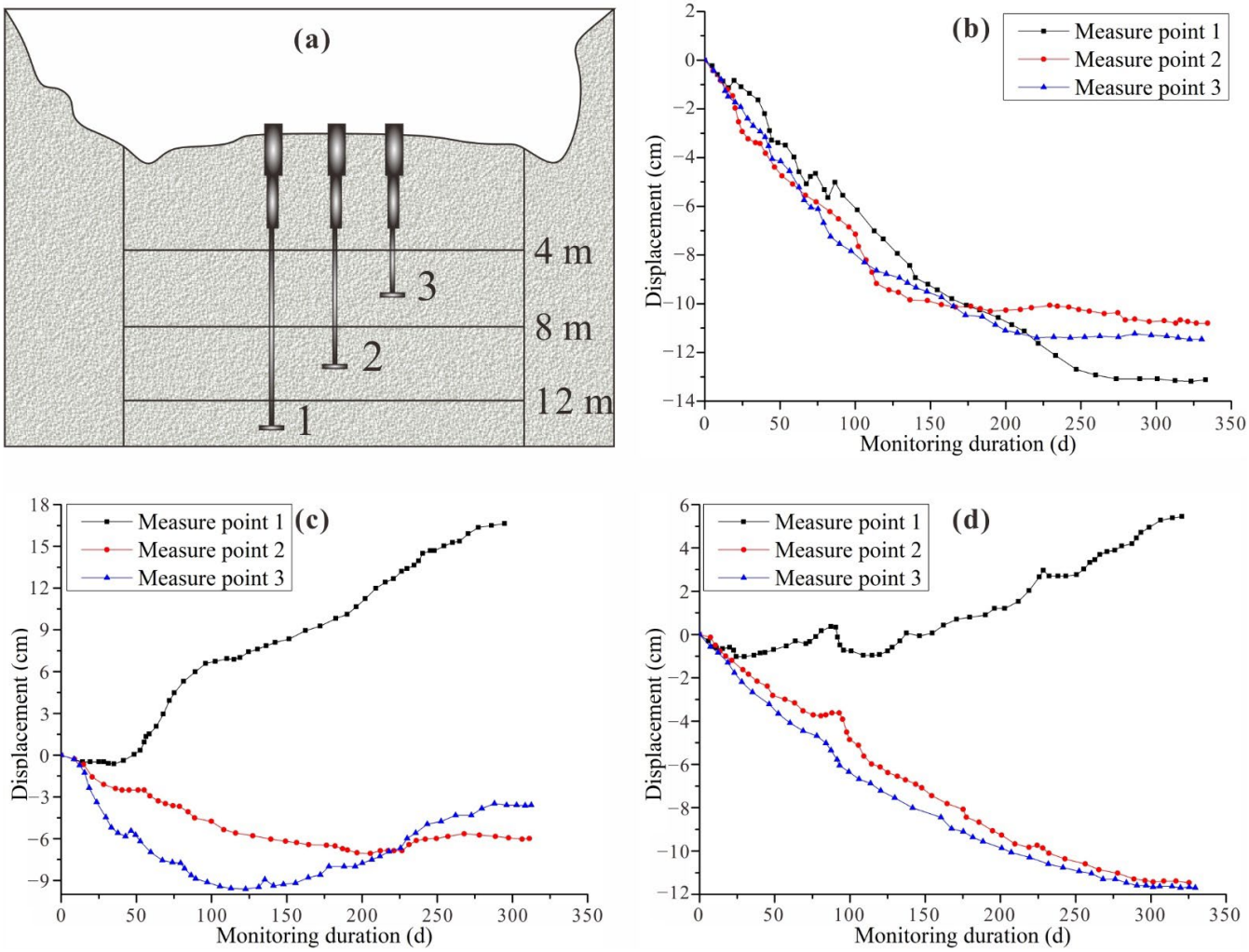

Figure 4. In situ deformation monitoring of the backfill. (**a**) Distribution of the displacement sensors; (**b**) Monitoring results of line 42; (**c**) Monitoring results of line 44; (**d**) Monitoring results of line 46.

As shown in the figures, for the backfill in line 42, the deformations of each layer are basically the same at the initial stage of monitoring, which all show compression deformation; that is to say, the backfill is uplifted as a whole. In the first 200 days of monitoring, the deformation was large, the deformation speed gradually decreased, and the backfill tended to be stable after 200 days. The largest deformation, which was about 13 cm, developed in the lower layer backfill.

The deformation law of the backfill body in line 44 is obviously different from that in line 42. From the beginning of monitoring, the changes in displacement of each measuring point were not synchronous. The lower filling layer shifted downward, while the upper filling layer moved upward, which resulted in a prominent bed-separation phenomenon. During the monitoring period of more than 300 days, the lower backfill continued to sink,

and the speed gradually slowed down. The maximum deformation value was about 17 cm when it finally reached stability. After rising for about 225 days, the filling body in the middle layer showed a slight decline. The upper filling body was uplifted continuously in the first 125 days, with a maximum uplift of about 9 cm, and then decreased until it achieved stability. Finally, the filling body presented a three-layer separation state.

The deformation trend of the filling body in line 46 was similar to that in line 44. Overall, the upper and middle filling layers were uplifted, while the lower filling layer sank. The difference is that the upper filling body of line 46 continued to be uplifted until it was stable, without a subsidence trend. During the monitoring time, the uplifts of the upper and middle backfill layers were each about 11 cm, and the maximum subsidence of the lower backfill layer was about 6 cm.

4. Numerical Simulation

The numerical simulation method is one of the most important research methods in mine engineering. Compared with field monitoring, numerical simulation is effective, adjustable, repeatable, and visible, which can also provide support for on-site monitoring [35,36].

4.1. Model Building

Based on the engineering geological conditions of the study area, a large three-dimensional numerical model was established using a multi-software modeling method. In model building, the convenient plane graph-editing function of CAD, the rich 3D-modeling function of Rhino, the powerful mesh splitting function of ANSYS, and the excellent calculation function of FLAC^{3D} were fully used to ensure the rationality and reliability of the results.

The model has a size of 3000 m × 3000 m × 800 m, with elevations of 1750 m at the top and 950 m at the bottom, as shown in Figure 5a. It can be seen from Figure 5b–d that the numerical model simulates the mine structure and geological conditions well. There are 137,511 nodes and 807,657 grids in the model. The Z direction in the model is upright, the X direction is the ore-body strike, and the Y direction is the ore-body dipping direction. The model contains four kinds of rock—the surrounding rock, rich ore, poor ore, and backfill—and their physical and mechanical parameters are presented in Table 1. The horizontal displacement on the left and right sides and the vertical displacement on the bottom are limited. The gradient in situ stresses are applied in the model, and the ground stress in the study area is calculated as follows:

$$\begin{aligned} \sigma_H &= 1.083 + 0.034Hg \\ \sigma_V &= 0.028H - 2.131 \end{aligned} \quad (1)$$

where σ_H is the horizontal geostress (MPa), σ_V is the vertical geostress (MPa), and H is the burial depth (m).

Table 1. Rock and backfill mechanical parameters in mining area No. 3.

Type	Density (g·cm^{-3})	Tensile Strength (MPa)	Compressive Strength (MPa)	Cohesion (MPa)	Internal Friction Angle (°)	Elastic Moduli (GPa)	Poisson's Ratio
Surrounding rock	2.6	12.2	152	13.5	35	64	0.28
Rich ore	3.05	0.5	16.4	4.6	41.7	8.6	0.31
Poor ore	3.02	0.5	17.2	5.2	42.2	8.8	0.22
Backfill	2	0.800	9.900	0.95	38	7.28	0.32

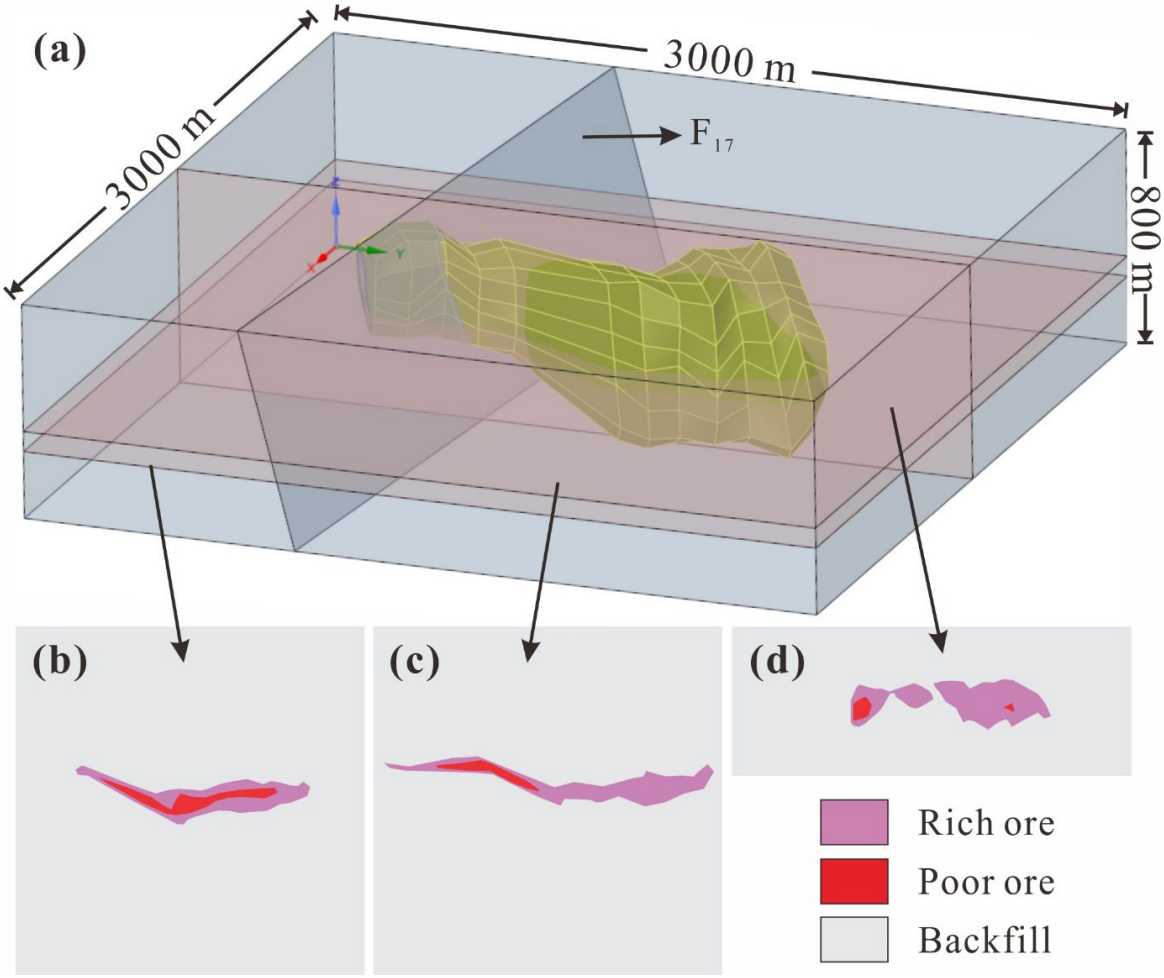

Figure 5. Numerical model. (**a**) Overall division of the model; (**b**) horizontal section of +1200 m; (**c**) horizontal section of +1275 m; (**d**) typical longitudinal section.

4.2. Numerical Simulation Results of Surface Subsidence

The model is excavated and filled according to the mining steps shown in Figure 2. For conveniently observing the displacement locations, the main lines and faults in the mining area are marked on the figures, as shown in Figure 6a. Surface settlement after each step of excavation is shown in Figure 6b–f.

After the first two steps of excavation, a settlement center is generated on line 54, with a maximum settlement of about 2 cm. According to the simulation results, the rock mass movement caused by underground mining forms an approximately circular area of movement after being transferred to the surface. The obvious settlement is located directly above the ore body, and there is a slight uplift around the model boundaries. The overall deformation in the mining area is not large.

In the third step, a large range of ore bodies on the east of the fault is mined. The surface settlement center moves toward the hanging wall of the ore body and gradually approaches line 42. The uplifted areas in the model all change to subsidence, indicating that the influence of mining on the surrounding environment is increasing, and the maximum subsidence is about 26 cm.

After the fourth step of excavation and filling, the settlement center moves to line 42, which is the same as the field monitoring result, and the maximum settlement is about 31 cm. Meanwhile, a large settlement area is developed on the footwall, and the mining area shows a tendency of a double settlement center.

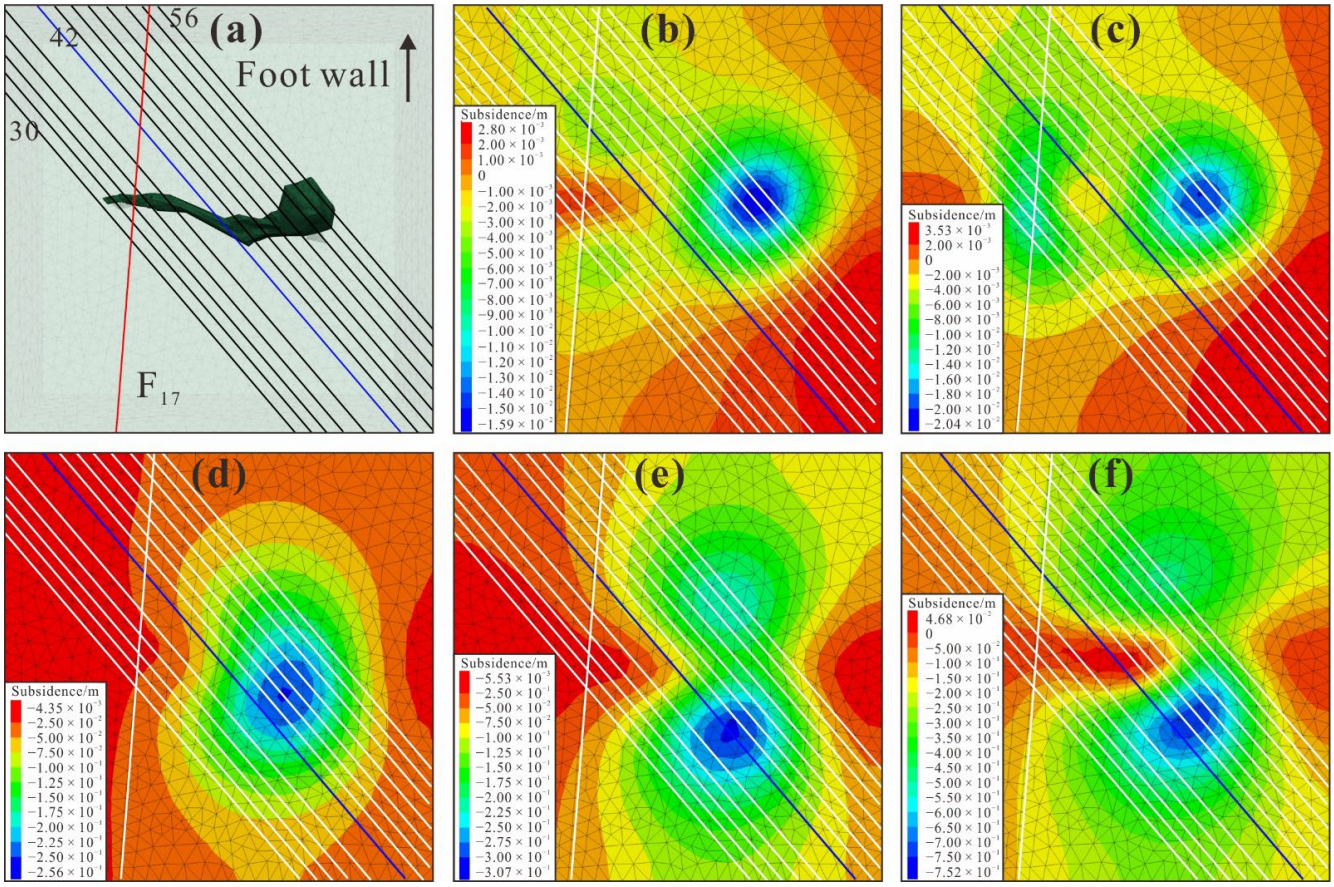

Figure 6. Numerical simulation results of surface subsidence. (**a**) Landmark location description; (**b**) surface deformation after the first mining step; (**c**) surface deformation after the second mining step; (**d**) surface deformation after the third mining step; (**e**) surface deformation after the fourth mining step; (**f**) surface deformation after the fifth mining step.

In the fifth step, the method consisting of the simultaneous mining of three sections is adopted. The distribution law of the surface settlement is similar to that in the fourth step, but the surface uplift occurs again just above the orebody. The surface subsidence increases greatly after this mining step. The main subsidence center on the hanging wall is located near line 44, and the subsidence is about 75 cm. The secondary subsidence on the footwall exceeds 50 cm, indicating that the multi-stage filling mining creates a significant disturbance in the rock mass in the mining area.

4.3. Numerical Simulation Results of Backfill Deformation

Figure 7 shows the simulation results of the filling body's deformation. To highlight the influence of the triple sub-level mining adopted in the fifth step, the filling body deformation results of the first four steps and the fifth step are compared. The fifth step of mining is carried out five times, and the ore body with a thickness of 10 m is mined each time. As can be seen from the figure, along the orebody strike direction, two wings of the backfill sink and the middle part of the backfill are uplifted. With continuous excavation and filling, the vertical displacement increases gradually, and the maximum deformation reaches about 61 cm. By comparing the sectional drawings of the filling body in the two stages, the internal deformation is larger than the external deformation, due to which the external filling body is restricted by the surrounding rock. In addition, because the strength of the filling body is low and easy to compress, the largest uplift point moves along the direction of the orebody to the thickest backfill layer. Meanwhile, in the vertical direction, the largest uplift point moves from the lower layer up to the middle layer. This indicates

that when the filling body is thin, its deformation will not be too large under the control of the surrounding rock. When the filling body is thick, the deformation caused by external stress will also be gradually absorbed by itself. A large uplift deformation is most likely developed in the backfill with moderate thickness under a thin overlying surrounding rock.

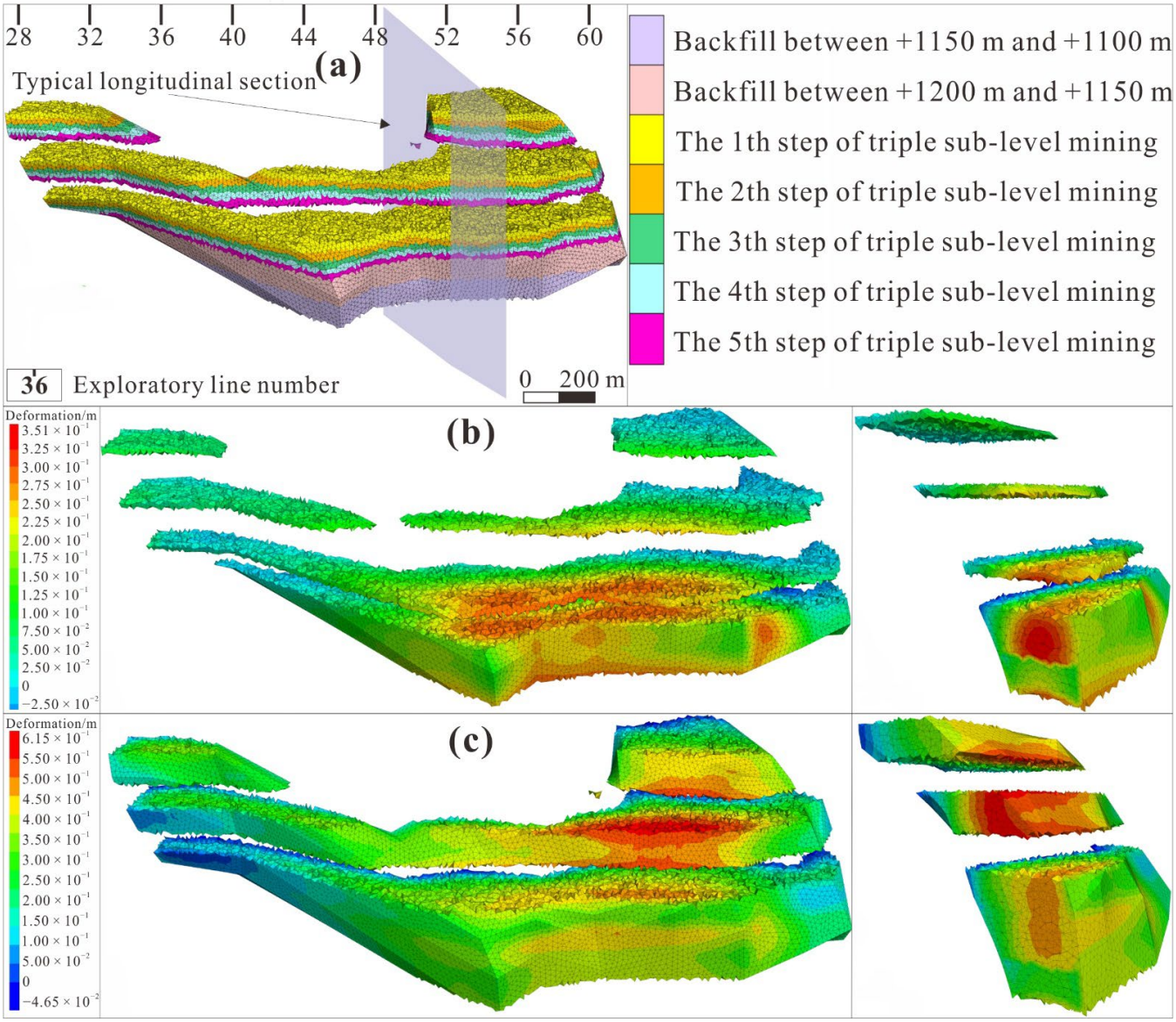

Figure 7. Numerical simulation results of backfill deformation. (**a**) Schematic diagram of filling body in each layer; (**b**) backfill deformation after the fourth mining step; (**c**) backfill deformation after the fifth mining step.

4.4. Numerical Simulation Analysis of a Typical Section

To reproduce the filling mining process in detail, a typical section was selected, and the meshes were refined as much as the computational efficiency allowed. The model has a size of 650 × 300 m, with elevations of +1750 m at the top and +1100 m at the bottom, and is divided into square grids with a side length of 5 m. The height of the mining approach is 5 m, and the backfill deformation process under the condition of the third middle section mining in step 5 is shown in Figure 8.

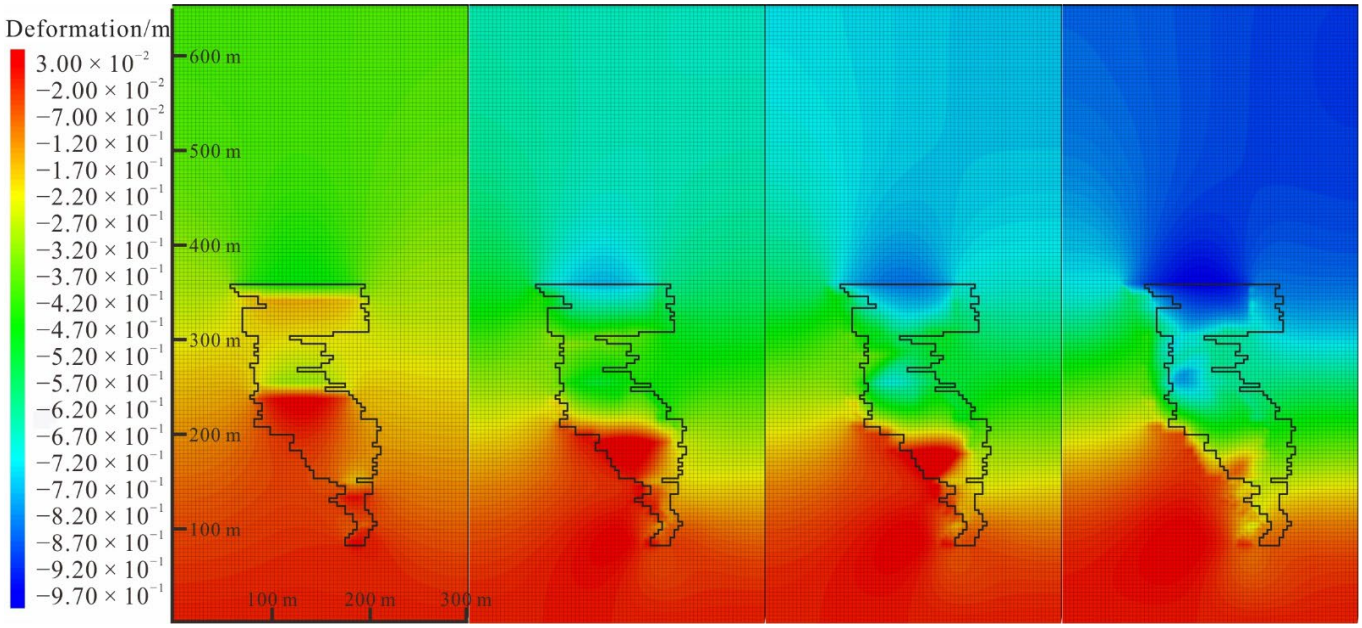

Figure 8. Numerical simulation results of the typical section.

It can be seen from the figure that the main deformation of the surrounding rock is subsidence. Uplift deformation only occurs under the goaf of each layer, which is caused by the floor-heaving of the backfill under the action of horizontal tectonic stress. This phenomenon is very common in deep mines. With the development of mining, the roof of the uppermost backfill body undergoes obvious subsidence, and the subsidence decreases with the extension to the surface. Furthermore, the subsidence on the hanging wall and footwall of the ore body differs. The surface deformation lags behind the filling body's roof deformation, and the settlement of the hanging wall is larger than that of the footwall. The shallow filling body mainly sinks under the action of gravity, while the deep filling body rises under the influence of horizontal tectonic stress, and the filling body shrinks inward as a whole. In addition, due to the different strengths of the backfill and the surrounding rock, the uneven deformation will lead to failure near the contact zone of the two materials.

5. Discussion

5.1. Comparison of the Results of On-Site Monitoring and Numerical Simulation

By comparing the surface subsidence results of numerical simulation and field monitoring, the surface deformation distribution law from the two methods has a good similarity, but there is also a certain difference in settlement amount, as shown in Table 2. The difference in magnitude may be affected by the following two reasons: Firstly, in the process of mining, both excavation and filling need a certain amount of time. The deformation of surrounding rock and the movement of the ground surface change with the construction time. However, numerical simulation can hardly reflect the time effect completely. Secondly, the causes of surrounding rock and surface deformation in the mining area are complicated, among which mining and filling constitute only one of the important factors. In addition, filling technology, blasting disturbance, groundwater, roadway support, etc. will all have an impact on it. It is difficult to consider all factors in numerical simulation, so a certain gap between the simulated data and the measured data is formed.

Table 2. Comparison of on-site monitoring results and simulation calculation results after each stage.

Mining Step	Year	Field Monitoring (m)	Numerical Simulation (m)	Difference (m)
1	2002	-	0.016	-
2	2005	0.026	0.020	0.006
3	2012	0.415	0.256	0.159
4	2017	0.613	0.307	0.306
5	2019	0.739	0.381	0.358
	2029	-	0.750	-

In order to accurately predict the ground subsidence induced by multi-stage filling mining based on the numerical model, a one-time function is obtained by fitting the difference between the measured value and the simulated value, as shown in Figure 9. The linear function is $y = 0.02533x - 50.79652$, and the fitting degree exceeds 0.99. According to the fitting curve, it can be calculated that the difference value is 0.598 m when the third middle section mining is completed in 2029, so the settlement value of the surface subsidence center is about 1.35 m. Overall, the range of surface deformation will further expand, and the settlement value of the subsidence center will increase steadily. The law of surface rock movement has not changed significantly and the settlement center has not shifted seriously, so it can be considered that the mining area is still in a relatively stable state.

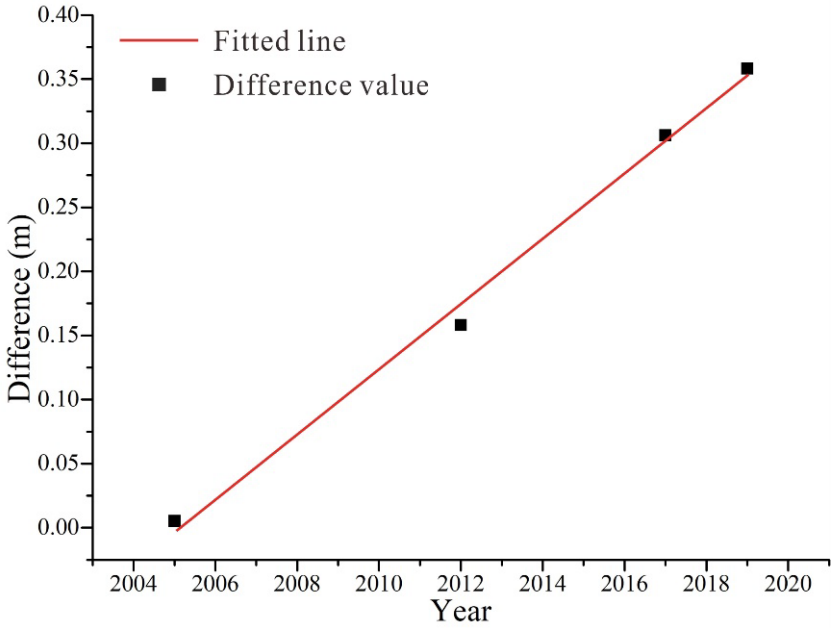

Figure 9. Fitting curve for the difference between the measured value and the simulated value.

5.2. Deformation Mechanism of the Backfill

After the filling body is filled into the goaf, it provides support for the surrounding rock deformation after a period of consolidation. In other words, the resistance provided by backfill is caused by the compression deformation of itself, which is a type of passive support. Figure 10 shows a simplified schematic diagram of backfill stress deformation, which consists of two parts: self-deformation and disturbance deformation. Self-deformation includes volume shrinkage, compression deformation, and roof-connected and bed separation. The bed separation is caused by the horizontal tectonic stress perpendicular to the ore body in the mining area squeezing the filling body, resulting in a certain bending deformation in the banded filling body. Disturbance deformation is mainly caused by the mutual dislocation of the filling body and the surrounding rock. In the horizontal direction,

the backfill body mainly shrinks inward, and the external deformation on the contact zone with the surrounding rock is larger than the internal deformation. In the vertical direction, the deformation is mainly manifested as the internal uplift and external subsidence, and the external deformation is smaller due to the restriction of the surrounding rock. The deformation of the surrounding rock has a certain lag compared with that of the backfill, and the internal deformation of the filling body is larger than that of the surrounding rock. Therefore, damage can easily develop around the backfill-surrounding rock contact zone due to uneven deformation.

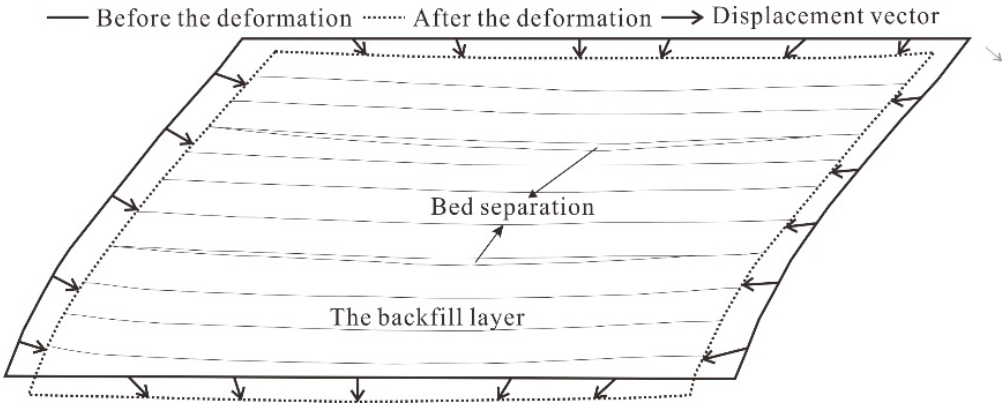

Figure 10. Deformation characteristic of a large volume of backfill.

6. Conclusions

The main conclusions of the research are as follows.

1. Through the use of GNSS monitoring for many years, the mechanisms of the surface deformation in the Jinchuan No.3 mining area are analyzed. Surface deformation is mainly affected by underground mining, and a settlement funnel is formed on the ground. With continuous mining and filling, the radius of the funnel gradually expands. The settlement near the orebody is obviously larger than that far away from the orebody, and the maximum subsidence reaches 739 mm in 14.5 years. The location of the settlement center exhibits an obvious movement toward the surface above the footwall of the ore body.
2. The influence of mining in the third section of the surface deformation is very significant, which is far greater than that of mining in the double section and the single section. In addition, the trend of surface movement is predicted. The single subsidence center on the upper wall develops into a double subsidence center, and the maximum value of the surface subsidence reaches about 1.35 m. Overall, the range of surface deformation will further expand, and the settlement value of the subsidence center will increase steadily. The law of surface rock movement has not changed significantly, and the settlement center has not shifted seriously, so the mining area can be considered to still be in a relatively stable state.
3. Based on the displacement monitoring data of the underground backfill, the deformation characteristics of the filling body are summarized. The whole filling body presents obvious subsidence, which is the main cause of ground settlement. With the development of multi-stage mining and filling, bed separation phenomena are found between the filling layers, and the closer to the interior, the more obvious it becomes.
4. The subsidence characteristics of the backfill are similar to those at the surface; that is, both the subsidence amount and speed are higher on the hanging wall than that on the footwall. Additionally, the backfill subsidence is slow and gradual, without sudden instability. In terms of the allowable space for deformation, the mass instability of the backfill is difficult. What needs to be considered is the influence of large-scale deformation on the mining and overlying strata, as well as the local deformation near the rock contact zone surrounding the backfill.

Author Contributions: Data curation, G.L.; formal analysis, Y.W. and J.G.; methodology, G.L. and Y.W.; software, G.L. and H.Z.; writing—original draft, G.L.; writing—review and editing, G.L. and F.M.; experiments, G.L., J.G. and Z.L. All authors have read and agreed to the published version of the manuscript.

Funding: This research was supported by the National Natural Science Foundation of China (Grant Nos. 42072305, 41877274, and 41831293).

Institutional Review Board Statement: Not applicable.

Informed Consent Statement: Not applicable.

Data Availability Statement: No new data were created or analyzed in this study. Data sharing is not applicable to this article.

Acknowledgments: The authors would like to express their sincere gratitude to Jinchuan Mine for their data support. In addition, the authors are grateful to assigned editors and anonymous reviewers for their enthusiastic help and valuable comments which have greatly improved this paper.

Conflicts of Interest: The authors declared that they have no conflict of interest regarding this study. We declare that we do not have any commercial or associative interests that represent a conflict of interest in connection with the paper submitted.

References

1. Li, G.; Wang, Z.; Ma, F.; Guo, J.; Liu, J.; Song, Y. A case study on deformation failure characteristics of overlying strata and critical mining upper limit in submarine mining. *Water* **2022**, *14*, 2465. [CrossRef]
2. Li, G.; Ma, F.; Guo, J.; Zhao, H. Deformation Characteristics and Control Method of Kilometer-Depth Roadways in a Nickel Mine: A Case Study. *Appl. Sci.* **2020**, *10*, 3937. [CrossRef]
3. Liu, J.; Ma, F.; Li, G.; Guo, J.; Wan, Y.; Song, Y. Evolution Assessment of Mining Subsidence Characteristics Using SBAS and PS Interferometry in Sanshandao Gold Mine, China. *Remote Sens.* **2022**, *14*, 290. [CrossRef]
4. Deng, X.; Zhang, J.; Kang, T.; Han, X. Strata behavior in extra-thick coal seam mining with upward slicing backfilling technology. *Int. J. Min. Sci. Technol.* **2016**, *26*, 587–592. [CrossRef]
5. Tang, Y.; Zheng, J.; Guo, L.; Zhao, Y. Effect of gypsum addition on the mechanical and microstructural performance of sulphide-rich cemented paste backfill. *Minerals* **2021**, *11*, 283. [CrossRef]
6. Ding, K.; Ma, F.; Guo, J.; Zhao, H.; Lu, R.; Liu, F. Investigation of the Mechanism of Roof Caving in the Jinchuan Nickel Mine, China. *Rock Mech. Rock Eng.* **2018**, *51*, 1215–1226. [CrossRef]
7. Du, Q.; Guo, G.; Li, H.; Gong, Y. Spatio-Temporal Evolution Law of Surface Subsidence Basin with Insufficient Exploitation of Deep Coal Resources in Aeolian Sand Area of Western China. *Remote Sens.* **2022**, *14*, 2536. [CrossRef]
8. Usanov, S.V.; Mel'Nik, V.V.; Zamyatin, A.L. Monitoring rock mass transformation under induced movements. *J. Min. Sci.* **2014**, *49*, 913–918. [CrossRef]
9. Herrera, G.; Tomás, R.; Lopez-Sanchez, J.M.; Delgado, J.; Mallorqui, J.J.; Duque, S.; Mulas, J. Advanced D In SAR analysis on mining areas: La Union case study (Murcia, SE Spain). *Eng. Geol.* **2007**, *90*, 148–159. [CrossRef]
10. Unlu, T.; Akcin, H.; Yilmaz, O. An integrated approach for the prediction of subsidence for coal mining basins. *Eng. Geol.* **2013**, *166*, 186–203. [CrossRef]
11. Jianjun, S.; Chunjian, H.; Ping, L.; Junwei, Z.; Deyuan, L.; Minde, J.; Lin, Z.; Jingkai, Z.; Jianying, S. Quantitative prediction of mining subsidence and its impact on the environment. *Int. J. Min. Sci. Technol.* **2012**, *22*, 69–73. [CrossRef]
12. Zhou, D.; Wu, K.; Li, L.; Diao, X.; Kong, X. A new methodology for studying the spreading process of mining subsidence in rock mass and alluvial soil: An example from the Huainan coal mine, China. *Bull. Eng. Geol. Environ.* **2016**, *75*, 1067–1087. [CrossRef]
13. Nicieza, C.G.; Fernandez, M.I.A.; Diaz, A.M.; Vigil, A.E.A. The new three-dimensional subsidence influence function denoted by n-k-g. *Int. J. Rock Mech. Min. Sci.* **2005**, *42*, 372–387. [CrossRef]
14. Díaz-Fernández, M.E.; Álvarez-Fernández, M.I.; Álvarez-Vigil, A.E. Computation of influence functions for automatic mining subsidence prediction. *Comput. Geosci.* **2010**, *14*, 83–103. [CrossRef]
15. Ma, F.; Zhao, H.; Yuan, R.; Guo, J. Ground movement resulting from underground backfill mining in a nickel mine (Gansu Province, China). *Nat. Hazards* **2015**, *77*, 1475–1490. [CrossRef]
16. Dussauge, C.; Grasso, J.R.; Helmstetter, A. Statistical analysis of rockfall volume distributions: Implications for rockfall dynamics. *Geophys. Res. Solid Earth* **2003**, *108*, 1–11. [CrossRef]
17. Ma, F.; Zhao, H.; Zhang, Y.; Guo, J.; Wei, A.; Wu, Z.; Zhang, Y. GPS monitoring and analysis of ground movement and deformation induced by transition from open-pit to underground mining. *J. Rock Mech. Geotech. Eng.* **2012**, *4*, 82–87. [CrossRef]
18. Nan, S.; Li, W.; Guan, W.; Liu, H.; Zhao, H.; Wen, Y.; Yao, J. Research on the Rapid Strengthening Mechanism of Microwave Field-Controlled Gypsum-Cemented Analog Materials. *Minerals* **2021**, *11*, 1348. [CrossRef]
19. Wu, J.; Feng, M.; Chen, Z.; Mao, X.; Han, G.; Wang, Y. Particle size distribution effects on the strength characteristic of cemented paste backfill. *Minerals* **2018**, *8*, 322. [CrossRef]

20. Lu, R.; Ma, F.S.; Guo, J.; Zhao, H.J. Monitoring and analysis of ground subsidence and backfill stress distribution in Jinchuan Mine, China. *Curr. Sci.* **2018**, *115*, 1970–1977. [CrossRef]
21. Yang, X.; Pang, J.; Liu, D.; Liu, Y.; Tian, Y.; Ma, J.; Li, S. Deformation mechanism of roadways in deep soft rock at Hegang Xing'an coalmine. *Int. J. Min. Sci. Technol.* **2013**, *23*, 307–312. [CrossRef]
22. Wang, M.; Guo, G.; Wang, X.; Guo, Y.; Dao, V. Floor heave characteristics and control technology of the roadway driven in deep inclined-strata. *Int. J. Min. Sci. Technol.* **2015**, *25*, 267–273. [CrossRef]
23. Chang, Q.L.; Zhou, H.Q.; Xie, Z.H.; Shen, S.P. Anchoring mechanism and application of hydraulic expansion bolts used in soft rock roadway floor heave control. *Int. J. Min. Sci. Technol.* **2013**, *23*, 323–328. [CrossRef]
24. Zhao, H.; Ma, F.; Zhang, Y.; Guo, J. Monitoring and mechanisms of ground deformation and ground fissures induced by cut-and-fill mining in the Jinchuan Mine 2, China. *Environ. Earth Sci.* **2013**, *68*, 1903–1911. [CrossRef]
25. Haslinda, N.; Sam, C.; Afshin, A.; Zainnuddin, M.D.; Bujang, K.H. Effect of inundation on shear strength characteristics of mudstone backfill. *Eng. Geol.* **2013**, *158*, 48–56.
26. Woo, K.; Eberhardt, E.; Elmo, D.; Stead, D. Empirical investigation and characterization of surface subsidence related to block cave mining. *Int. J. Rock Mech. Min. Sci.* **2013**, *61*, 31–42. [CrossRef]
27. Mohammadali, S.; Apel, D.B.; Hall, R.A. Prediction of mininginduced surface and ground movements at a Canadian diamond mine using an elastoplastic finite element model. *Int. J. Rock Mech. Min. Sci.* **2017**, *100*, 73–82.
28. Uibu, M.; Somelar, P.; Raado, L.; Irha, N.; Hain, T.; Koroljova, A.; Kuusik, R. Oil shale ash based backfilling concrete-strength development, mineral transformations and leachability. *Constr. Build. Mater.* **2016**, *102*, 620–630. [CrossRef]
29. Aldhafeeri, Z.; Fall, M. Time and damage induced changes in the chemical reactivity of cemented paste backfill. *J. Environ. Chem. Eng.* **2016**, *4*, 4038–4049. [CrossRef]
30. Chen, X.; Guo, H.; Zhao, P.; Peng, X.; Wang, S. Numerical modeling of large deformation and nonlinear frictional contact of excavation boundary of deep soft rock tunnel. *J. Rock Mech. Geotech. Eng.* **2011**, *3*, 421–428.
31. Li, G.; Ma, F.; Guo, J.; Zhao, H.; Liu, G. Study on deformation failure mechanism and support technology of deep soft rock roadway. *Eng. Geol.* **2020**, *264*, 105262. [CrossRef]
32. Li, G.; Ma, F.S.; Guo, J.; Zhao, H. Experimental research on deformation failure process of roadway tunnel in fractured rock mass induced by mining excavation. *Environ. Earth Sci.* **2022**, *82*, 243. [CrossRef]
33. Yang, Z.Q. Key technology research on the efficient exploitation and comprehensive utilization of resources in the deep Jinchuan nickel deposit. *Engineering* **2017**, *3*, 559–566. [CrossRef]
34. Li, G.; Ma, F.S.; Guo, J.; Zhao, H. Case study of roadway deformation failure mechanisms: Field investigation and numerical simulation. *Energies* **2021**, *14*, 1032. [CrossRef]
35. Li, G.; Ma, F.; Liu, G.; Zhao, H.; Guo, J. A Strain-Softening Constitutive Model of Heterogeneous Rock Mass Considering Statistical Damage and Its Application in Numerical Modeling of Deep Roadways. *Sustainability* **2019**, *11*, 2399. [CrossRef]
36. Chen, L.; Fan, G.; Zhang, D.; Fan, Z.; Wang, X.; Zhang, W.; Yao, N. Numerical Simulation of Crack Initiation and Propagation Evolution Law of Hydraulic Fracturing Holes in Coal Seams Considering Permeability Anisotropy and Damage. *Minerals* **2022**, *12*, 494. [CrossRef]